HHS Public Access

Author manuscript

Nature. Author manuscript; available in PMC 2017 May 09.

Published in final edited form as:

Nature. 2016 November 17; 539(7629): 428–432. doi:10.1038/nature20145.

Neuromodulators signal through astrocytes to alter neural circuit activity and behavior

Zhiguo Ma[1], **Tobias Stork**[1], **Dwight E. Bergles**[2], and **Marc R. Freeman**[1,3,*]

[1] Department of Neurobiology and Howard Hughes Medical Institute, University of Massachusetts Medical School, Worcester, MA 01605, USA

[2] Solomon H. Snyder Department of Neuroscience, Johns Hopkins University School of Medicine, Baltimore, MD 21205, USA

Summary

Astrocytes associate with synapses throughout the brain and express receptors for neurotransmitters that can elevate intracellular calcium (Ca^{2+}) [1-3]. Astrocyte Ca^{2+} signaling has been proposed to modulate neural circuit activity [4], but pathways regulating these events are poorly defined and *in vivo* evidence linking changes in astrocyte Ca^{2+} to alterations in neurotransmission or behaviors is limited. Here we show *Drosophila* astrocytes exhibit activity-regulated Ca^{2+} signaling events *in vivo*. Tyramine (Tyr) and octopamine (Oct) released from $Tdc2^{+}$ neurons signal directly to astrocytes to stimulate Ca^{2+} increases through the octopamine-tyramine receptor (Oct-TyrR) and the TRP channel Waterwitch (Wtrw), and astrocytes in turn modulate downstream dopaminergic (DA) neurons. Tyr or Oct application to live preparations silenced dopaminergic (DA) neurons and this inhibition required astrocytic Oct-TyrR and Wtrw. Increasing astrocyte Ca^{2+} signaling was sufficient to silence DA neuron activity, which was mediated by astrocyte endocytic function and adenosine receptors. Selective disruption of Oct-TyrR or Wtrw expression in astrocytes blocked astrocyte Ca^{2+} signaling and profoundly altered olfactory-driven chemotaxis behavior and touch-induced startle responses. Our work identifies Oct-TyrR and Wtrw as key components of the astrocyte Ca^{2+} signaling machinery, provides direct evidence that Oct- and Tyr-based neuromodulation can be mediated by astrocytes, and demonstrates that astrocytes are essential for multiple sensory-driven behaviors.

Astrocytes are intimately associated with brain synapses and positioned to broadly regulate synaptic activity. It has been widely proposed that astrocytes modulate neural circuits and behavior [5-7], although *in vivo* data demonstrating astrocytes are directly activated by neurotransmission and signal back to neurons to modulate output remains elusive.

*Correspondence to freemmar@ohsu.edu.

[3]Current address: Vollum Institute, Oregon Health and Sciences University, Portland, OR 97239, USA

Author Information

The authors state that they have no competing financial interests.

Statement of Individual Contributions

ZM and MRF designed most experiments. ZM performed all experiments. TS provided *alrm-LexA::GAD* transgenic flies. AS generated *pUAST-wtrw::gfp* construct. ZM and MRF wrote the manuscript with editing by TS.

Astrocytes exhibit dynamic fluctuations in intracellular Ca^{2+} *in vitro* [8,9] and *in vivo* [10,11] suggesting Ca^{2+} signaling might be a useful measure of astrocyte "activity". Despite decades of studies on astrocytic Ca^{2+} transients, signaling pathways controlling these transients remain poorly defined, and their *in vivo* relevance remains controversial. If astrocytes indeed actively participate in information processing in circuits, it is imperative we characterize such mechanisms as they would represent a potentially widespread mechanism for controlling brain function.

We performed an RNAi-based screen in *Drosophila* where we individually knocked-down ~500 Ca^{2+} signaling-related genes selectively in astrocytes using the astrocyte-specific *Gal4* driver line *alrm-Gal4* [12], and assayed larval olfactory-driven chemotaxis behavior (Extended Data Fig. 1a). We found astrocyte knockdown of the TRP channel Water witch (Wtrw)[13] led to a significant (~50%) decrease in larval chemotaxis toward iso-amyl acetate (IAA)(Fig. 1a). Similar results were found with a second, non-overlapping RNAi construct (Fig. 1a) and was specific to glia as shown by insensitivity to blockade of Gal4/UAS in neurons with *elav-Gal80* (Extended Data Fig. 1e). The null allele $wtrw^{ex}$ was equally defective in chemotaxis, which was rescued by re-expression of *wtrw* only in astrocytes (Fig. 1a). We also found that blockade of Gal4/UAS driven $wtrw^{RNAi}$ with *tsh-Gal80* in the ventral nerve cord (VNC) resulted in normal chemotaxis responses (Extended Data Fig. 1f), revealing a critical role for VNC astrocytes in this behavior, although this does not exclude an additional role for brain astrocytes. Chemotaxis defects did not result from simple alterations in motility, as $wtrw^{RNAi}$ animals exhibited normal locomotion (Extended Data Fig. 1g) and light avoidance responses (Extended Data Fig. 1c,h). We conclude that Wtrw is required in astrocytes for normal larval olfactory-driven behavior.

Ca^{2+} transients in mammalian astrocytes in awake behaving mice are induced during periods of elevated arousal [14-16]. We therefore used a gentle anterior touch assay[17] to examine the role of astrocyte Ca^{2+} signaling in larval startle-induced behaviors. Crawling larvae touched anteriorly with a hair responded by pausing and continuing forward (Type I response), or by moving backward and executing an escape response (Type II response) (Extended Data Fig. 1b). Control animals exhibited roughly equal frequencies of Type I and Type II responses, however, $wtrw^{RNAi}$ in astrocytes resulted in a dramatic alteration in behavior: ~80% of larvae exhibited Type I responses, a phenomenon mimicked by $wtrw^{ex}$ mutants (Fig. 1b) and the phenotype is independent of neurons (Extended Data Fig. 1i). These data indicate astrocyte expressed Wtrw also modulates startle-induced behavioral changes in *Drosophila* larvae.

To explore *in vivo* Ca^{2+} signaling we developed a semi-dissected preparation to image the larval central nervous system (CNS). GCaMP6s was used to image astrocyte cytosolic Ca^{2+} changes (UAS-GCaMP6s), mCherry (UAS-mCherry) was used as a reference for astrocyte position, and dorsal astrocyte cell bodies were imaged in the VNC. We found astrocyte cell bodies exhibited coordinated, population-wide slow oscillations (termed somatic Ca^{2+} transients) (Extended Data Fig. 1j-I; Supplementary video 1). Somatic Ca^{2+} transients occurred approximately every 2 minutes and exhibited an average ~11% change in dF/F (Extended Data Fig. 1m). Interestingly, blocking neuronal activity with tetrodotoxin (TTX) suppressed transients by approximately 60%, as did application of the broad Ca^{2+} channel

blocker lanthanum chloride ($LaCl_3$)(Extended Data Fig. 1n). Similar astrocyte Ca^{2+} transients were observed when we imaged intact immobilized larvae (Extended Data Fig. 1o), indicating our dissected preparation preserves *in vivo* patterns of astrocyte activity.

TRP channels regulate Ca^{2+} levels in astrocytes [18], we therefore reasoned Wtrw might drive Ca^{2+} signaling in *Drosophila* astrocytes. Control larvae exhibited 8-9 rhythmic oscillations in somatic Ca^{2+} transients over 15 minutes. In contrast, astrocyte-specific $wtrw^{RNAi}$ led to a roughly 50% decrease in somatic astrocyte Ca^{2+} transients, which was also observed in the $wtrw^{ex}$ mutant (Fig. 1c). Bath application of acetylcholine, glutamate, and γ-aminobutyric acid in the presence of TTX did not elicit a change in Ca^{2+} levels in astrocytes. In contrast, application of tyramine (Tyr) or octopamine (Oct), the invertebrate analogues of norepinephrine, which has been shown to induce Ca^{2+} transients in mammalian astrocytes [14,15,19,20], potently elevated somatic Ca^{2+} levels in astrocytes (Fig. 1d), indicating astrocyte somatic Ca^{2+} signaling is regulated by these neuromodulators.

$Tdc2^+$ neurons are the only known source of Tyr and Oct in the larval VNC [21]. To explore their relationship with astrocytes we expressed the red-shifted Ca^{2+} indicator R-GECO1 in $Tdc2^+$ neurons (using *tdc2-LexA/LexAop-R-GECO1*) and GCaMP6s in astrocytes (using *alrm-Gal4/UAS-GCaMP6s*) and examined *in vivo* activity. We observed a striking positive correlation between $Tdc2^+$ neuron activity and somatic astrocyte Ca^{2+}: when $Tdc2^+$ neurons were active, astrocyte somatic Ca^{2+} levels increased, and when $Tdc2^+$ neurons were silent, astrocyte somatic Ca^{2+} levels decreased (Fig. 2a; Supplementary video 2). A similar correlation was observed in intact larvae (Extended Data Fig. 1p). Moreover, the amplitude and duration of somatic astrocyte Ca^{2+} rise was tightly correlated with Ca^{2+} spikes in $Tdc2^+$ neurons (Fig. 2a). When we chronically silenced $Tdc2^+$ neurons by expressing the K^+ leak channel Kir2.1[22], rhythmic oscillations in astrocyte Ca^{2+} were eliminated (Fig. 2b; Extended Data Fig. 2a); and acute optogenetic blockade of $Tdc2^+$ neuron activity using halorhodopsin (*tdc2-Gal4>UAS-NpHR*) led to a decrease in astrocyte somatic Ca^{2+} (Fig. 2c; Extended Data Fig. 2b). Interestingly, astrocyte Ca^{2+} signaling was also blocked by the α1 adrenergic receptor antagonist terazosin (Fig. 2d; Extended Data Fig. 2c), which inhibits arousal-evoked Ca^{2+} responses in cortical astrocytes in mammals [14,15], further supporting the notion that astrocyte modulation is highly conserved between species. Consistent with astrocyte Ca^{2+} signaling being regulated by Oct and Tyr, we found somatic astrocyte Ca^{2+} transients were nearly absent (~80% reduced) in $tdc2^{RO54}$ mutants, which lack both Tyr and Oct, although they persisted in $tβh^{nM18}$ mutants, which lack Oct but retain Tyr signaling (Fig. 2e,f). Finally, $Tdc2^+$ neurons were activated when olfactory neurons were optogenetically stimulated in intact larvae (using *or83b-Gal4*), suggesting sensory cues flow to $Tdc2^+$ neurons, which are upstream of astrocyte Ca^{2+} signaling (Extended Data Fig. 2d).

To determine whether $Tdc2^+$ neurons signal directly to astrocytes we knocked down the two Tyr receptors TyrR and TyrRII, and Oct-TyrR, a dual specificity receptor capable of binding both Oct and Tyr [23,24], in astrocytes and assayed Ca^{2+} signaling. Depletion of TyrR or TyrRII had no effect (Data not shown), however depletion of Oct-TyrR strongly suppressed astrocyte somatic Ca^{2+} transients. We observed strong inhibition of astrocyte somatic Ca^{2+} transients in the $Oct\text{-}TyrR^{hono}$ homozygous mutant, and in $Oct\text{-}TyrR^{hono/+}$ heterozygous mutants, which were previously shown to have dominant effects [25] (Fig. 2g). Loss of one

copy of *Oct-TyrR* (*Oct-TyrR*^{hono}/+) also led to deficits in chemotaxis behavior similar to those observed with astrocyte-specific knockdown of *wtrw*; these behavioral changes were enhanced in the *Oct-TyrR*^{hono} homozygous mutant, or by astrocyte-specific knockdown of *Oct-TyrR* with two copies of an *Oct-TyrR* RNAi construct. Co-expression of *Oct-TyrR*^{RNAi} and *wtrw*^{RNAi}, did not enhance chemotaxis defects, suggesting they act in a common genetic pathway (Fig. 2h). Finally, astrocyte-specific depletion of Oct-TyrR led to a strong inhibition of Type II escape responses in the gentle anterior touch assay (Fig. 2i). We conclude Wtrw and Oct-TyrR are required in astrocytes to trigger somatic Ca^{2+} transients in response to Oct and Tyr, and astrocyte Wtrw and Oct-TyrR are essential for normal olfactory-driven chemotaxis and startle-induced escape responses.

Astrocytes support neuronal function in many ways and it is plausible that alterations in astrocyte Ca^{2+} signaling might modify upstream $Tdc2^{+}$ neuron firing to influence behaviors. We therefore examined the frequency and amplitude of firing events in $Tdc2^{+}$ neurons in *wtrw*^{ex} null mutants and found no alterations compared to controls (Extended Data Fig. 2e). That $Tdc2^{+}$ neurons fire normally in *wtrw* mutants indicates that blocking astrocyte Ca^{2+} signaling does not lead to a global disruption of neuronal activity in the larval CNS.

Biogenic amines often regulate dopaminergic (DA) neurons [26]. Triple labeling revealed that astrocytes, $Tdc2^{+}$ neurons and DA neurons are in close proximity in the larval CNS (Extended Data Fig. 2f). When we imaged DA neuron activity (using *th-Gal4*/*UAS-GCaMP6s*) we found *wtrw*^{ex} mutants exhibited a significant increase (~50-70%) in the frequency of DA Ca^{2+} transients in multiple segmental clusters of TH^{+} cells. A similar phenotype was observed in *Oct-TyrR*$^{hono/+}$ mutants (Fig. 3a), although there were no significant changes in the average amplitude of DA neuron responses (Extended Data Fig. 2g). Thus Wtrw and Oct-TyrR negatively regulate DA neuron firing. Consistent with this observation, we found bath application of Oct or Tyr, but not vehicle (DMSO) to larval CNS suppressed DA neuron activity within seconds (Fig. 3b). Strikingly, depletion of the Oct-TyrR and Wtrw specifically from astrocytes using RNAi potently suppressed Tyr-induced Ca^{2+} elevation in astrocytes and silencing of DA neurons (Fig. 3c; Extended Data Fig. 2k). These data indicate that Tyr signals through astrocyte Oct-TyrR and Wtrw to inhibit downstream DA neuron activity. To explore how DA neuron modulation regulates larval chemotaxis behavior we performed a series of acute manipulations. We first expressed the temperature sensitive channel TrpA1 in DA neurons and found after 24-hour ectopic activation of DA neurons larvae exhibited profound chemotaxis defects similar to those observed when Wtrw or Oct-TyrR were depleted from astrocytes (Extended Data Fig. 2h). In addition, feeding larvae a dopamine D1-like receptor antagonist rescued deficits associated with *wtrw*^{RNAi} in astrocytes in chemotaxis assays (Extended Data Fig. 2i). These data support the notion that the increased DA neuron activity observed after depletion of astrocyte Oct-TyrR and Wtrw is responsible for defects in chemotaxis behavior.

How do astrocytes regulate DA neuron firing? Astrocytic release of ATP and signaling through purinergic receptors is one mechanism by which astrocytes appear to modulate neuronal activity [27,28]. The *Drosophila* genome contains a single seven transmembrane purinergic receptor, AdoR, that is most similar to mammalian adenosine receptors [29]. Pretreatment of larval CNS preparations with the AdoR antagonist SCH-442416 blocked

Tyr-induced DA neuron silencing without altering overall DA neuron activity before Tyr treatment. Similar results were observed in AdoR null mutants (Fig. 4a; Extended Data Fig. 2j). Purinergic signaling often results from vesicular release of ATP, which can be hydrolyzed to adenosine by ectoenzymes. We manipulated exocytosis selectively in astrocytes using a dominant negative version of the dynamin Shibire (Shi^{DN}) and found this suppress the ability of Tyr to silence DA neurons. This blockade was not enhanced further by application of AdoR antagonists and had no effect on baseline DA neuron activity before Tyr treatment (Fig. 4b; Extended Data Fig. 2l). Finally, to determine whether astrocyte Ca^{2+} signaling through TRP channels is sufficient to suppress DA neuron firing we expressed the wasabi (AITC)-sensitive *Drosophila* TrpA1 channel in astrocytes and assayed the effects of AITC application on astrocyte Ca^{2+} signaling and DA neuron firing. Exposure of control animals to AITC did not alter astrocyte Ca^{2+} levels, however application of AITC to preparations expressing TrpA1 in astrocytes led to an increase in GCaMP6s signals of astrocytes of ~20% (Extended Data Fig. 2m), similar to that elicited by Tyr application (Fig. 1d). Moreover, AITC activation of astrocyte Ca^{2+} signaling resulted in a strong suppression of DA neuron activity. This effect was reversible by application of AdoR antagonists and did not occur when AITC was applied to control (i.e. non-TrpA1 expressing) animals (Fig. 4c; Extended Data Figure 2n). Thus TrpA1 channel mediated increases in astrocyte Ca^{2+} signaling are sufficient to silence DA neurons *in vivo*. DA neuron silencing is likely be mediated by ATP release from astrocytes and subsequent activation of AdoR on DA neurons.

It has been assumed that neuromodulators alter neural circuit activity and behaviors by directly acting on neurons; however, astrocytes (and other glia) express a diverse array of neuromodulatory receptors suggesting they may contribute to the global effects of these neurotransmitters. In this study we show neuromodulatory signaling in at least some cases flows through astrocytes. We demonstrate *Drosophila* astrocytes exhibit robust Ca^{2+} signaling events remarkably similar to those observed in awake behaving mice [14-16]. Similar to the global activation of astrocyte Ca^{2+} signaling by norepinephrine in mammals, release of tyramine (and likely octopamine) *in vivo* triggers synchronous activation of astrocytes. We identify Wtrw and Oct-TyrR as key components of the astrocyte Ca^{2+} signaling axis and their loss of function phenotypes provide direct evidence that astrocyte Ca^{2+} signaling modulates animal behaviors. Furthermore, we show that during suppression of DA neuron activity, Oct/Tyr signal directly to astrocytes, and astrocyte Ca^{2+} transients execute neuromodulatory events downstream (Fig. 4d). Octopamine and tyramine have been linked to arousal and aggression in insects and are considered to be functionally equivalent to norepinephrine in mammals. The profound modulation of astrocyte Ca^{2+} levels by norepinephrine in mammals [14-16] suggests that the Tyr/Oct/norepinephrine-mediated activation of astrocyte Ca^{2+} signaling, and in turn astrocyte-based neuromodulation, are ancient features of the metazoan nervous system. A reassessment of the cellular basis of neuromodulation is therefore warranted, with further reflection on direct roles for astrocytes in transducing neuromodulatory signals in neural circuits.

Material and Methods

Fly stocks and husbandry

Flies were cultured in standard cornmeal food at 25°C in 12h/12h light/dark cycles. Fly stocks include: *w^{1118}*, *alrm-Gal4* [26], *alrm-LexA::GAD*, *UAS-wtrw-gfp*, *LexAop-R-GECO1* (Bloomington, *52224*), *tdc2-Gal4* (Bloomington, *9313*), *20XUAS-IVS-GCaMP6s* (Bloomington, *42746*), *13XLexAop2-IVS-GCaMP6s-p10* (Bloomington, *44274*), *UAS-Kir2.1-EGFP* (Bloomington, *6595*), *UAS-Oct-$TyrR^{RNAi}$* (Bloomington, *28332*), *th-Gal4* (Bloomington, *8848*), *UAS-$wtrw^{VDRC}$* (VDRC, *107423*), *Oct-$TyrR^{hono}$* (Kyoto, *109038*), *UAS-shi^{DN}* (Bloomington, *5822*), *UAS-TrpA1* (Bloomington, *26263*), *UAS-NpHR* (Kyoto, *117008*), *UAS-CsChrimson* (Bloomington, *55135*), *$AdoR^{KG03964ex}$* (Bloomington, *30868*), *tdc2-LexA::p65* [27], *UAS-$wtrw^{2.23}$* [28], *$wtrw^{ex}$* [29], *$tβh^{nM18}$* [30], *$tdc2^{RO54}$* [31], *th-LexA::p65* [32], *tsh-Gal80* [33].

Behavioral tests

Chemotaxis and phototaxis—These two assays were performed using protocols described previously with minor modifications [34]. Briefly, pools of ~100 3rd instar larvae (108-120h after egg lay) were allowed to freely move for 5 minutes on petri dishes with according settings for chemotaxis assay or phototaxis assay, then the numbers of larvae in odorant/vehicle circles, or in light/dark quadrants were scored respectively. Response indices were calculated as: $RI_{chemotaxis}=(N_{odor}-N_{vehicle})/(N_{odor}+N_{vehicle})$, $RI_{phototaxis}=(N_{dark}-N_{light})/(N_{dark}+N_{light})$. Isoamyl acetate (IAA) was diluted to 1:5000 in mineral oil, and pure mineral oil was used as the control. Light intensity in phototaxis assays was 2400 lux white light (5400K). Thermogenetic manipulation of dopaminergic neurons was accomplished by transferring 3rd instar larvae from 18°C to 25°C to allow activation of TrpA1 for 24h before testing. For chemotaxis assays related to D1-like or D2-like dopamine receptor inhibitors 3rd instar larvae were fed on cornmeal food mixed with inhibitors for 24h before testing.

Gentle touch assay—Adapted from [35], early 3rd instar larvae (84-96h after egg lay) were struck in the thoracic segments with a hair while moving straight. No response, a stop, head retraction and turn were grouped into type I response, initiation of at least one single full body retraction or multiple full body retractions were categorized as type II reversal responses.

Larval motility—3rd instar larvae (108-120h after egg lay) were videotaped and the maximal velocity was calculated by dividing the travel distance measured when larvae move straight without pause by time.

Molecular biology and transgenic flies

pUAST-wtrw::gfp was made by cloning full length *wtrw* tagged with *gfp* at C terminal into *pUAST*. Transgenic flies were obtained by standard germline injection (BestGene Inc, Chino Hills, CA).

Chemicals, buffers and antibodies

For live preparation studies all the chemicals were diluted in live imaging buffer (110mM NaCl, 5.4mM KCl, 1.2mM $CaCl_2$, 0.8mM $MgCl_2$, 10mM D-glucose, 10 mM HEPES, pH adjusted to 7.2), including 1μM tetrodotoxin, 0.1mM $LaCl_3$, 2.5mM octopamine, 2.5mM glutamate, 2.5mM acetylcholine, 2.5mM GABA, 150μM AITC, 10μM SCH-442416, 1mM terazosin, 0.5mM tyramine was used unless otherwise stated. 0.2mg/ml SCH-23390 (dopamine D1 like receptor antagonist), 0.2mg/ml Eticlopride (dopamine D2 like receptor antagonist), 10mM all trans retinal. Rabbit anti-GAT was used at 1:5000.

Live imaging and data analysis

1st instar larvae were immersed in halocarbon oil 27 and immobilized between coverslips and slides to image the activity of neurons and astrocytes through the cuticle in intact larvae. 3rd instar wandering stage larvae were used to dissect the CNS. Briefly, intact CNS were transferred to a silicon pad after dissection and incubated with 100μl live imaging buffer. Samples were allowed to sit at room temperature for 15 minutes before imaging. To examine the effects of lanthanum chloride ($LaCl_3$) or tetrodotoxin (TTX) on calcium transients, samples were pre-incubated in buffer containing chemicals for 15 minutes before imaging. Movies were acquired by using Volocity software on a spinning disc microscope equipped with a 20X (dissected CNS) or 40X (intact larvae) water immersion objective at 2 frames/second. Changes of GCaMP intensity of ROIs were calculated and expressed as $(F_{t1...n}\text{-}F)/F$ (first 10 frames were averaged as F), which then were plotted over time. Plotted traces were semi-automatically analyzed by the multiple peak fitting function of Igor Pro (WaveMetrics Inc., OR) to obtain the numbers and amplitudes of peaks.

Bath application of drugs

Samples were prepared as described above, incubated with imaging buffer (with/without 1μM TTX). At ~240s (astrocytes) or ~300s (neurons) after imaging, 100μl live imaging buffer containing 2X final concentrations of chemicals (with/without 1μM TTX) were directly added to the medium, and imaging continued. GCaMP6s intensity of ROIs were plotted and analyzed as mentioned above. For terazosin experiments we first examined preparations for 6 min (control, pre-exposure window), terazosin was perfused for 3 min, and we then imaged for an additional 6min (exposed window). Data points of 6-9min that represented the perfusion window were omitted in graph.

Optogenetic activation/inactivation of neurons

For CsChrimson activation of olfactory neurons larvae were grown on cornmeal food daily topped with 100 μl all trans retinal for 3 days. Early 3rd instar larvae were immobilized between coverslips and slides in halocarbon oil 27, activity of $Tdc2^+$ neurons reflected by GCaMP6s were continuously monitored except when red light (640nm, 3.41mW/ mm^2) was delivered through an epifluorescence light source. Halorhodopsin mediated inhibition of Tdc2 neurons was accomplished by growing larvae on cornmeal food topped daily with 100 μl all trans retinal for 4-5 days. Larval brains were dissected from wandering 3rd instar larvae and prepared as described above for imaging somatic calcium transients in astrocytes. GCamP6s signals were recorded for 6 minutes, then halorhodopsin was activated (within

~30 seconds) by alternating delivering 561nm (0.26mW/mm^2, 3s, for photoinhibition) and blue light 488nm (500msec, for imaging GCaMP6s labeled astrocytes) for another 6min. Data points from two consecutive movies were then assembled together to show changes of somatic calcium transients.

Statistical analysis

No statistical methods were used to predetermine sample size. All n numbers represent biological replicates. The experiments were not randomized or blinded. The Shapiro–Wilk test (normal distribution if $P>0.05$) was used to determine the normality of data. Statistical comparisons were performed using one-way ANOVA followed by Tukey's post hoc test or paired Student's *t*-test (two-tailed). Non-normally distributed data were compared using Wilcoxon and Mann-Whitney tests followed by *Bonferroni*-Holm post hoc test. *P* values less than 0.05 were considered significant. All the data in bar graphs are expressed as mean ± s.e.m.

Extended Data

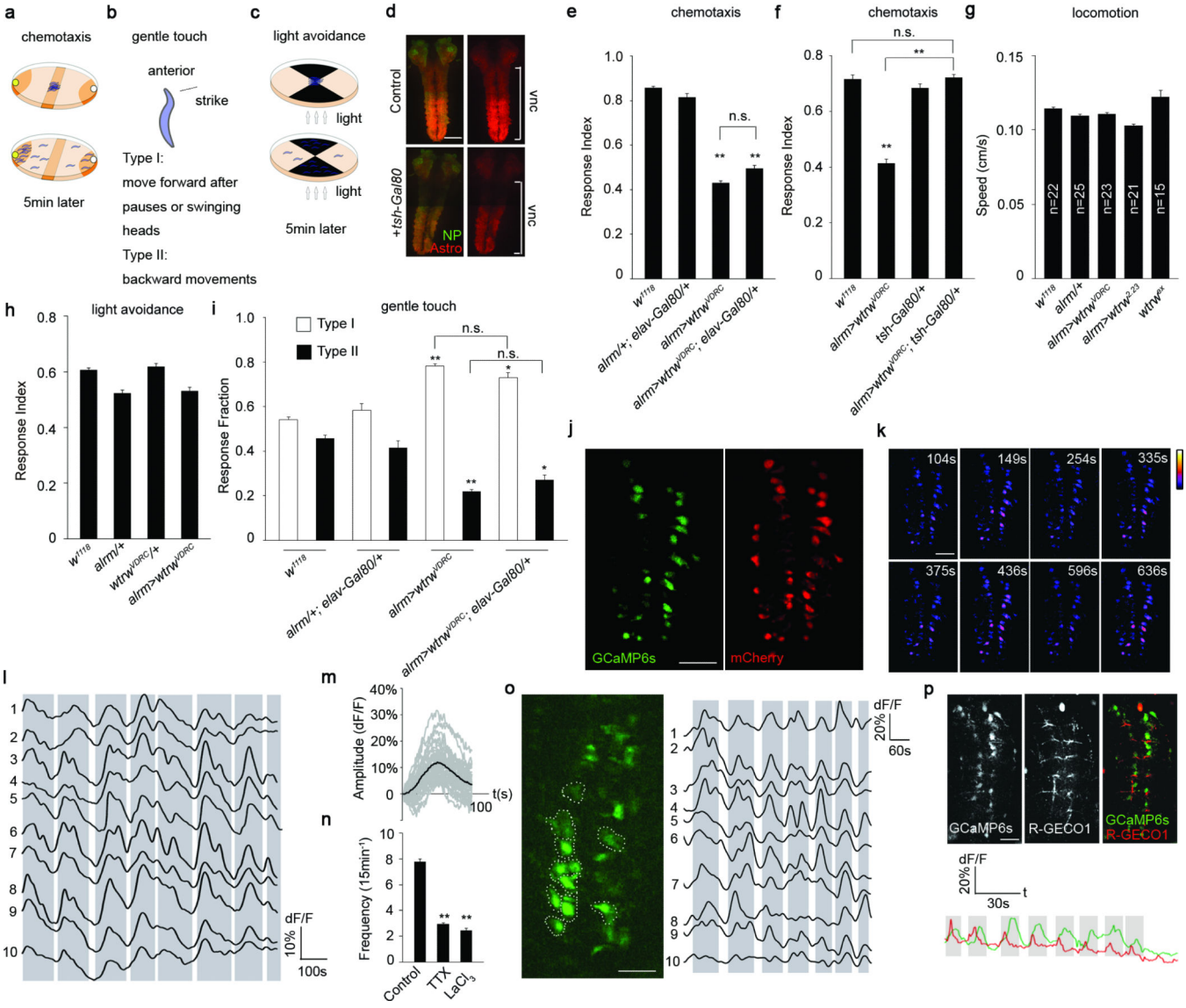

Extended Data Figure 1. Synchronous somatic Ca^{2+} transients in *Drosophila* astrocytes

a-c, Brief diagrams of behavioral tests. **d**, *tsh-Gal80* suppression of *alrm-Gal4* activity. Nc82, neuropil (NP). Astrocytes (Astro), *alrm>myr::mtdTomato*. Vnc, ventral nerve cord. Scale bar, 50μm. **e**,**f**, Chemotaxis assay (n=12). **g**, Locomotion assay (n listed). **h**, Light avoidance assay (n=12). **i**, Gentle touch assay (n=24). **j**, GCaMP6s and mCherry expression in astrocytes. Scale bar, 50μm. **k**, Representative pseudocolored images of 4 continuous Ca^{2+} transients. Scale bar, 50μm. **l**, Traces of normalized GCaMP6s intensity over mCherry of 10 individual astrocytes in 15min live imaging window. **m**, Averaged traces of individual somatic Ca^{2+} transients. **n**, somatic Ca^{2+} transients in astrocytes with treatments of TTX and $LaCl_3$ (n=10, 160 cells). **o**, GCaMP6s expression in astrocytes and traces of 10 individual astrocytes from an intact larva. Scale bar, 20μm. Grey bars (**l**,**o**) represent population rise/fall in GCaMP6s signals. **p**, GCaMP6s labeled astrocytes and R-GECO1 labeled $Tdc2^{+}$ neurites

and their averaged traces in an intact larva. Scale bar, 20μm. *p<0.05, **p<0.01, n.s., not significant. Error bar, s.e.m. Wilcoxon and Mann-Whitney tests followed by Bonferroni-Holm post hoc test (**e**,**n**), one-way ANOVA followed by Tukey's post hoc test (**f**,**g**,**h**,**i**).

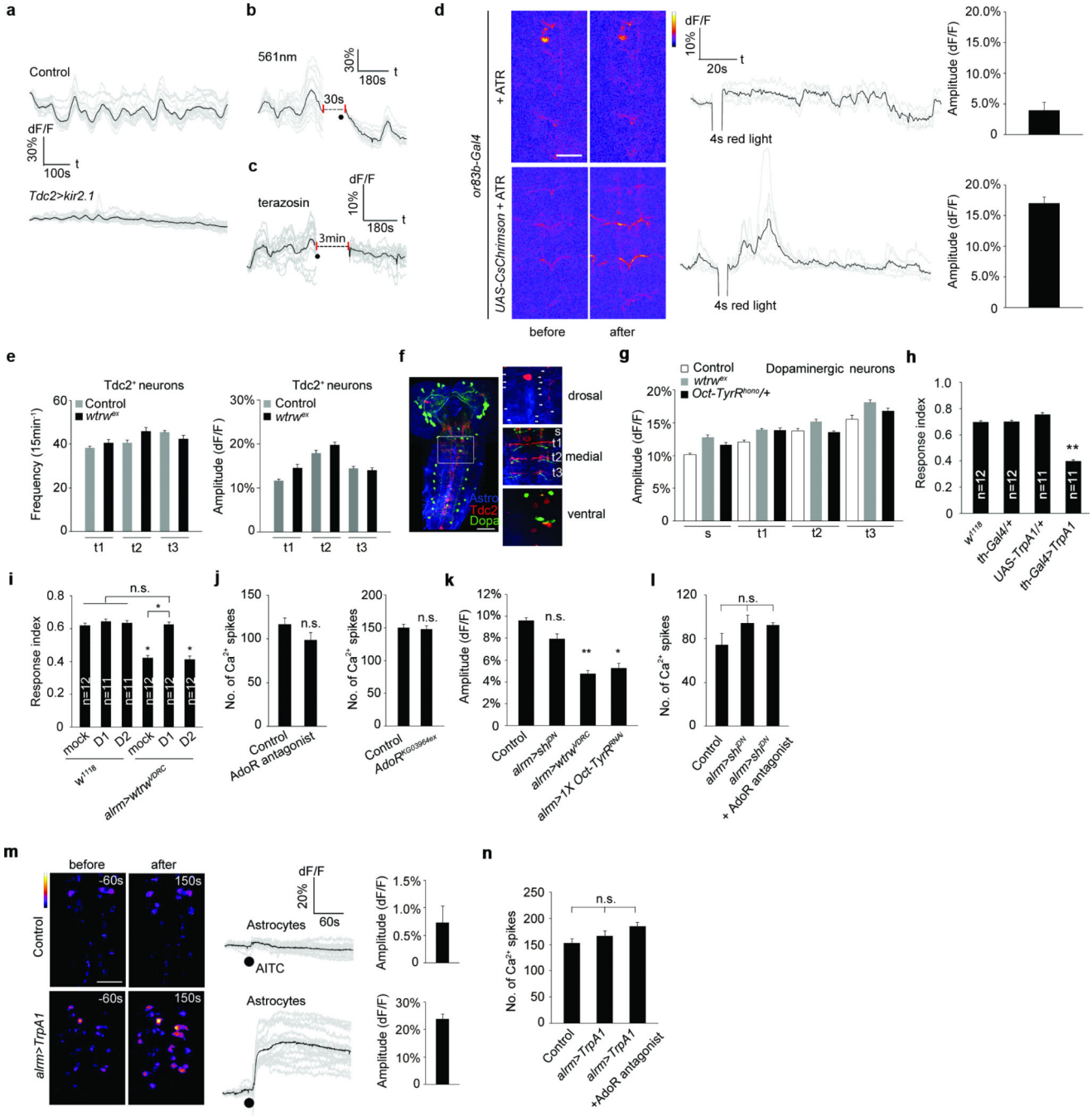

Extended Data Figure 2. Somatic Ca^{2+} transients of astrocytes inhibit the activity of dopaminergic neurons

a-c, Representative traces of astrocyte Ca^{2+} transients with blockade of tyramine/octopamine signaling. **d,** Stimulation of olfactory neurons activates $Tdc2^{+}$ neurons (n=3-4). Scale bar, 25μm. **e**, Activity of $Tdc2^{+}$ neurons are not altered in *wtrw* mutants (n=8, 48

neurites). **f**, Astrocytes, Tdc2^{+} neurons and dopaminergic neurons in larval CNS. Dorsal (arrows point to astrocyte somas), medial (neurites intermingled with ramified processes of astrocytes for monitoring activity are labeled) and ventral (cell bodies of Tdc2^{+} and dopaminergic neurons) images from the boxed region are shown right. s, subesophageal. t, thoracic. Scale bar, 50μm. **g**, Amplitude of Ca^{2+} spikes of dopaminergic neurons (n=10, 80 neurites). **h**,**i**, Chemotaxis assay (n listed). **j**, Number of Ca^{2+} spikes of dopaminergic neurons (n=6, 48 neurites). **k**, Responses of astrocytes to tyramine (0.5mM) in the presence of TTX (n=6, 96 cells total). **l**, Number of Ca^{2+} spikes of dopaminergic neurons (n=6, 48 neurites). **m**, AITC induces Ca^{2+} influx to astrocytes expressing TrpA1 (n=5, 80 cells). Scale bar, 50μm. **n**, Number of Ca^{2+} spikes of dopaminergic neurons (n=6, 48 neurites). *p<0.05, **p<0.01, n.s., not significant. Error bar, s.e.m. One-way ANOVA followed by Tukey's post hoc test.

Supplementary Material

Refer to Web version on PubMed Central for supplementary material.

Acknowledgements

We are grateful to colleagues, the Vienna Drosophila RNAi Center and the Bloomington Stock Center for generously providing fly stocks. We thank members of the Freeman lab for comments on the manuscript. This work was supported by NINDS grant R01 NS053538 (to MRF). During the period of this study MRF was an Investigator with the Howard Hughes Medical Institute.

References

1. Cornell-Bell AH, Finkbeiner SM, Cooper MS, Smith SJ. Glutamate induces calcium waves in cultured astrocytes: long-range glial signaling. Science. 1990; 247:470–473. [PubMed: 1967852]
2. Charles AC, Merrill JE, Dirksen ER, Sanderson MJ. Intercellular signaling in glial cells: calcium waves and oscillations in response to mechanical stimulation and glutamate. Neuron. 1991; 6:983–992. [PubMed: 1675864]
3. Dani JW, Chernjavsky A, Smith SJ. Neuronal activity triggers calcium waves in hippocampal astrocyte networks. Neuron. 1992; 8:429–440. [PubMed: 1347996]
4. Smith SJ. Do astrocytes process neural information? Prog. Brain Res. 1992; 94:119–136.
5. Khakh BS, McCarthy KD. Astrocyte Calcium Signaling: From Observations to Functions and the Challenges Therein. Cold Spring Harb Perspect Biol. 2015; 7:a020404. [PubMed: 25605709]
6. Araque A, et al. Gliotransmitters travel in time and space. Neuron. 2014; 81:728–739. [PubMed: 24559669]
7. Khakh BS, Sofroniew MV. Diversity of astrocyte functions and phenotypes in neural circuits. Nat. Neurosci. 2015; 18:942–952. [PubMed: 26108722]
8. Fatatis A, Russell JT. Spontaneous changes in intracellular calcium concentration in type I astrocytes from rat cerebral cortex in primary culture. Glia. 1992; 5:95–104. [PubMed: 1349589]
9. Nett WJ, Oloff SH, McCarthy KD. Hippocampal astrocytes in situ exhibit calcium oscillations that occur independent of neuronal activity. J. Neurophysiol. 2002; 87:528–537. [PubMed: 11784768]
10. Porter JT, McCarthy KD. Hippocampal astrocytes in situ respond to glutamate released from synaptic terminals. J. Neurosci. 1996; 16:5073–5081. [PubMed: 8756437]
11. Nimmerjahn A, Mukamel EA, Schnitzer MJ. Motor behavior activates Bergmann glial networks. Neuron. 2009; 62:400–412. [PubMed: 19447095]
12. Doherty J, Logan MA, Taşdemir OE, Freeman MR. Ensheathing glia function as phagocytes in the adult Drosophila brain. J. Neurosci. 2009; 29:4768–4781. [PubMed: 19369546]

13. Liu L, et al. Drosophila hygrosensation requires the TRP channels water witch and nanchung. Nature. 2007; 450:294–298. [PubMed: 17994098]
14. Ding F, et al. α1-Adrenergic receptors mediate coordinated Ca2+ signaling of cortical astrocytes in awake, behaving mice. Cell Calcium. 2013; 54:387–394. [PubMed: 24138901]
15. Paukert M, et al. Norepinephrine controls astroglial responsiveness to local circuit activity. Neuron. 2014; 82:1263–1270. [PubMed: 24945771]
16. Srinivasan R, et al. Ca(2+) signaling in astrocytes from Ip3r2(-/-) mice in brain slices and during startle responses in vivo. Nat. Neurosci. 2015; 18:708–717. [PubMed: 25894291]
17. Zhou Y, Cameron S, Chang W-T, Rao Y. Control of directional change after mechanical stimulation in Drosophila. Mol Brain. 2012; 5:39. [PubMed: 23107101]
18. Shigetomi E, Jackson-Weaver O, Huckstepp RT, O'Dell TJ, Khakh BS. TRPA1 channels are regulators of astrocyte basal calcium levels and long-term potentiation via constitutive D-serine release. J. Neurosci. 2013; 33:10143–10153. [PubMed: 23761909]
19. Duffy S, MacVicar BA. Adrenergic calcium signaling in astrocyte networks within the hippocampal slice. J. Neurosci. 1995; 15:5535–5550. [PubMed: 7643199]
20. Salm AK, McCarthy KD. Norepinephrine-evoked calcium transients in cultured cerebral type 1 astroglia. Glia. 1990; 3:529–538. [PubMed: 2148555]
21. Vömel M, Wegener C. Neuroarchitecture of aminergic systems in the larval ventral ganglion of Drosophila melanogaster. PLoS ONE. 2008; 3:e1848. [PubMed: 18365004]
22. Nitabach MN, Sheeba V, Vera DA, Blau J, Holmes TC. Membrane electrical excitability is necessary for the free-running larval Drosophila circadian clock. J. Neurobiol. 2005; 62:1–13. [PubMed: 15389695]
23. Saudou F, Amlaiky N, Plassat JL, Borrelli E, Hen R. Cloning and characterization of a Drosophila tyramine receptor. EMBO J. 1990; 9:3611–3617. [PubMed: 2170118]
24. Robb S, et al. Agonist-specific coupling of a cloned Drosophila octopamine/tyramine receptor to multiple second messenger systems. EMBO J. 1994; 13:1325–1330. [PubMed: 8137817]
25. Kutsukake M, Komatsu A, Yamamoto D, Ishiwa-Chigusa S. A tyramine receptor gene mutation causes a defective olfactory behavior in Drosophila melanogaster. Gene. 2000; 245:31–42. [PubMed: 10713442]
26. Burke CJ, et al. Layered reward signalling through octopamine and dopamine in Drosophila. Nature. 2012; 492:433–437. [PubMed: 23103875]
27. Newman EA. Glial cell inhibition of neurons by release of ATP. J. Neurosci. 2003; 23:1659–1666. [PubMed: 12629170]
28. Lalo U, Rasooli-Nejad S, Pankratov Y. Exocytosis of gliotransmitters from cortical astrocytes: implications for synaptic plasticity and aging. Biochem. Soc. Trans. 2014; 42:1275–1281. [PubMed: 25233403]
29. Brody T, Cravchik A. Drosophila melanogaster G protein-coupled receptors. J. Cell Biol. 2000; 150:F83–8. [PubMed: 10908591]

Materials and methods references

30. Doherty J, Logan MA, Taşdemir OE, Freeman MR. Ensheathing glia function as phagocytes in the adult Drosophila brain. J. Neurosci. 2009; 29:4768–4781. [PubMed: 19369546]
31. Burke CJ, et al. Layered reward signalling through octopamine and dopamine in Drosophila. Nature. 2012; 492:433–437. [PubMed: 23103875]
32. Liu L, et al. Drosophila hygrosensation requires the TRP channels water witch and nanchung. Nature. 2007; 450:294–298. [PubMed: 17994098]
33. Kim SH, et al. Drosophila TRPA1 channel mediates chemical avoidance in gustatory receptor neurons. Proc. Natl. Acad. Sci. U.S.A. 2010; 107:8440–8445. [PubMed: 20404155]
34. Monastirioti M, Linn CE, White K. Characterization of Drosophila tyramine beta-hydroxylase gene and isolation of mutant flies lacking octopamine. J. Neurosci. 1996; 16:3900–3911. [PubMed: 8656284]

35. Cole SH, et al. Two functional but noncomplementing Drosophila tyrosine decarboxylase genes: distinct roles for neural tyramine and octopamine in female fertility. J. Biol. Chem. 2005; 280:14948–14955. [PubMed: 15691831]

36. Galili DS, et al. Converging circuits mediate temperature and shock aversive olfactory conditioning in Drosophila. Curr. Biol. 2014; 24:1712–1722. [PubMed: 25042591]

37. Clyne JD, Miesenböck G. Sex-specific control and tuning of the pattern generator for courtship song in Drosophila. Cell. 2008; 133:354–363. [PubMed: 18423205]

38. Lilly M, Carlson J. smellblind: a gene required for Drosophila olfaction. Genetics. 1990; 124:293–302. [PubMed: 2106470]

39. Zhou Y, Cameron S, Chang W-T, Rao Y. Control of directional change after mechanical stimulation in Drosophila. Mol Brain. 2012; 5:39. [PubMed: 23107101]

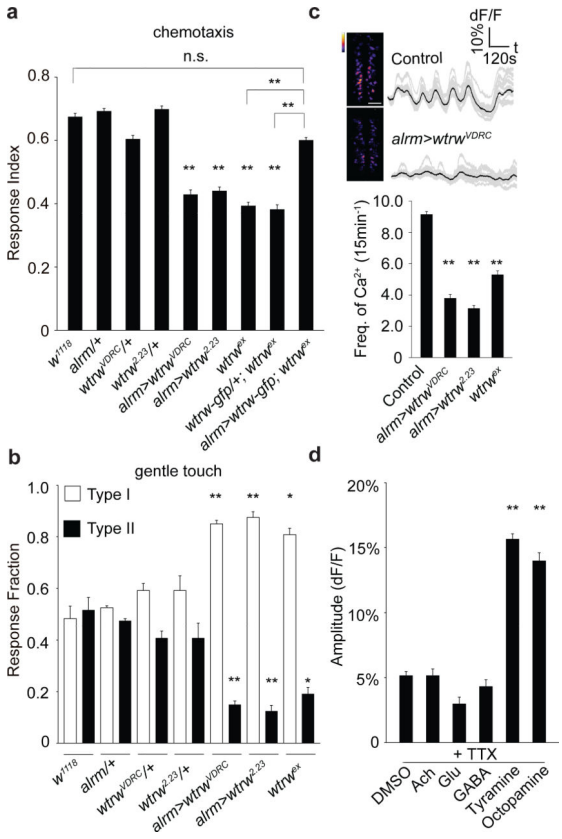

Figure 1. Larval chemotaxis and startle-induced responses require the astrocyte-expressed TRP channel Water witch

a, Chemotaxis assay (n=12). **b**, Gentle touch assay (n=30). **c**, Pseudocolored maximum intensity projections of 15min movies, averaged traces of 16 individual astrocytes and quantifications of the frequency of somatic Ca^{2+} transients (n=10, 160 cells total). Scale bar, 50μm. **d**, Responses of astrocytes to neurotransmitters/neuromodulators in the presence of tetrodotoxin (n=6, 96 cells total). *p<0.05, **p<0.01, n.s., not significant, Error bars, s.e.m. Wilcoxon and Mann-Whitney tests followed by Bonferroni-Holm post hoc test (**a**). One-way ANOVA followed by Tukey's post hoc test (**b**,**c**,**d**).

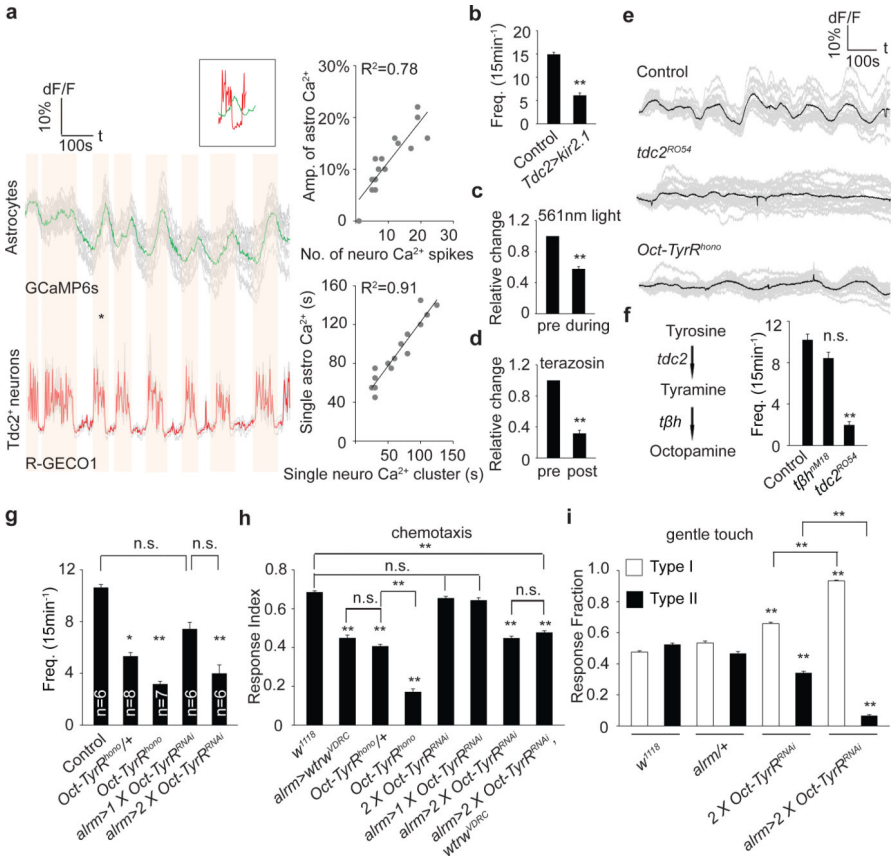

Figure 2. Tdc2^{+} neurons fire rhythmically to drive astrocyte somatic Ca^{2+} transients through the octopamine-tyramine receptor (Oct-TyrR)

a, Correlation analyses of neuronal activity and somatic Ca^{2+} transients in astrocytes. Averaged traces of 16 individual astrocytes (GCaMP6s) and 4 pairs of Tdc2^{+} neurites (R-GECO1) from the same sample. Vertical orange bars highlight concomitant activity in astrocytes and neurons (* marked events are shown in inset). Amplitude and duration of individual Ca^{2+} transients in astrocytes correlate highly with activity of Tdc2^{+} neurons. **b**, Frequency of Ca^{2+} transients in astrocytes (n=10,160 cells total). **c**,**d**, Relative changes in numbers of Ca^{2+} transients after acute blockade of octopamine/tyramine signaling by halorhodopsin (**c**) or terazosin (**d**) (n=6, 96 cells total). Black dots, when either 561nm light or terazosin was delivered. **e**, Representative traces of astrocytic Ca^{2+} transients in mutants defective in tyramine/octopamine signaling. **f**,**g**, Frequency of Ca^{2+} transients in *tdc2*^{RO54}, *tβh*^{nM18} (**f**, n=6, 96 cells total) and *Oct-TyrR*^{hono} mutants (**g,** n listed for each genotype, 16n cells total). **h**, Chemotaxis assay (n=12). **i**, Gentle touch assay (n=30). *p<0.05, **p<0.01, n.s., not significant. Error bar, s.e.m. Paired t-test (**c**,**d**), one-way ANOVA followed by Tukey's post hoc test (**b**,**f**,**g**,**h**,**i**).

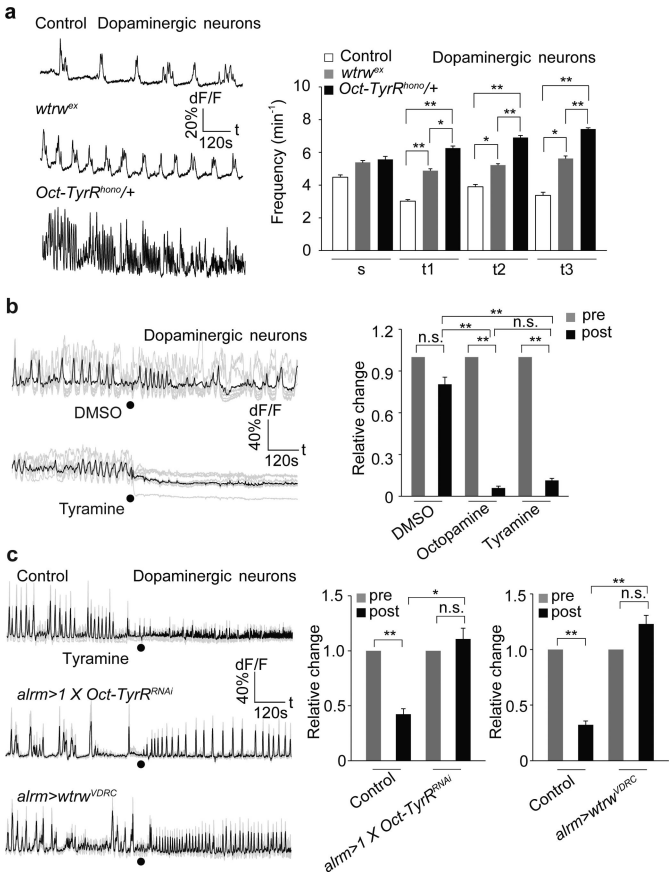

Figure 3. Astrocytes mediate tyramine-induced inhibition of dopaminergic neurons through Oct-TyrR

a, Enhanced activity of dopaminergic neurons in *wtrw*^{ex} mutant, *Oct-TyrR*^{hono}/+ heterozygotes (n=10, 80 neurites). s, subesophageal segments. t, thoracic segments. **b**, Tyramine and octopamine (2.5mM) inhibit the activity of dopaminergic neurons (n=6, 48 neurites). **c**, Astrocyte-specific RNAi for *Oct-TyrR* or *wtrw* attenuates inhibition of tyramine on dopaminergic neurons (n=6, 48 neurites). Black dots, when tyramine was perfused. **p*<0.05, ***p*<0.01, n.s., not significant. Error bar, s.e.m. Paired t-test (**b**, same treatment, **c**, same genotype), one-way ANOVA followed by Tukey's post hoc test (**a**,**b**,**c**).

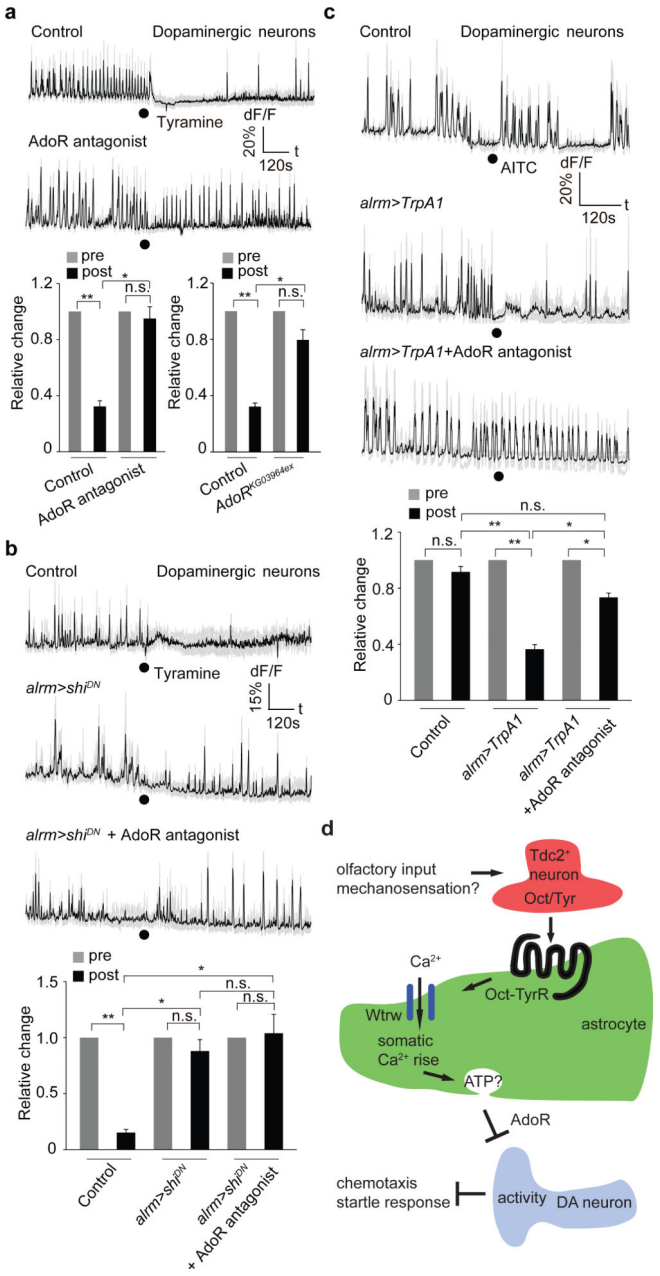

Figure 4. Tyramine mediated inhibition of dopaminergic neurons depends on adenosine receptor and glial endocytic function

a, AdoR is required for tyramine mediated inhibition of dopaminergic neurons (n=6, 48 neurites). **b,** Blockade of endocytic function by dominant negative shibire (shi^{DN}) attenuates inhibition of tyramine on dopaminergic neurons (n=6, 48 neurites). Black dots, when tyramine was perfused. **c**, Ca^{2+} influx to astrocytes through TrpA1 is sufficient to inhibit dopaminergic neurons (n=6, 48 neurites). Black dots, when AITC was perfused. **d**, Model. Olfactory and likely mechanosensory information flow towards Tdc2^{+} neurons that release Oct and Tyr to activate the Oct-TyrR on astrocytes and in turn astrocyte Ca^{2+} entry through the TRP channel Wtrw. Increase in astrocyte Ca^{2+} is sufficient to silence DA neurons through a mechanism requiring the adenosine receptor AdoR, potentially through astrocyte

ATP release and its breakdown to adenosine. Inhibition of DA neuron activity by astrocytes is essential for normal chemotaxis and startle-induced reversal behaviors. *p<0.05, **p<0.01, n.s., not significant. Error bar, s.e.m. Paired t test (**a**,**b**,**c**, same genotype), Wilcoxon and Mann-Whitney tests followed by Bonferroni-Holm post hoc test (**a**,**b**), one-way ANOVA followed by Tukey's post hoc test (**c**).